X-ray-Induced Production of Gold Nanoparticles on a SiO_2/Si System and in a Poly(methyl methacrylate) Matrix

Ferdi Karadas, Gulay Ertas, Eda Ozkaraoglu, and Sefik Suzer*

Bilkent University, Department of Chemistry, 06800 Ankara, Turkey

Received August 27, 2004. In Final Form: October 19, 2004

Prolonged exposure to X-rays of $HAuCl_4$ deposited from an aqueous solution onto a SiO_2/Si substrate or into a poly(methyl methacrylate) (PMMA) matrix induces reduction of the Au^{3+} ions to Au^0 and subsequent nucleation to gold nanoclusters as recorded by X-ray photoelectron spectroscopy. The corresponding major oxidation product is determined as chlorine $\{HAuCl_4(ads) + X\text{-rays} \rightarrow Au(ads) + (3/2)Cl_2(ads) + HCl(ads)\}$, which is initially adsorbed onto the surface but eventually diffuses out of the system into the vacuum. The reduced gold atoms aggregate (three-dimensionally) into gold nanoclusters as evidenced by the variation in the binding energy during X-ray exposure, which starts as 1.3 eV but approaches a value that is 0.5 eV higher than that of the bulk gold. The disappearance of the oxidation product (Cl2p signal) and the growth of the nanoclusters (related to the measured binding energy difference between the Si2p of the oxide and Au4f of the reduced gold) exhibit first-order kinetics which is approximately 3 times slower than the reduction of Au^{3+}, indicating that both of the former processes are diffusion controlled. Similarly, gold ions incorporated into PMMA can also be reduced and aggregated to gold nanoclusters using 254 nm deep UV irradiation in air evidenced by UV−vis−NIR absorption spectrocopy.

Introduction

Preparation of metal nanoparticles on various substrates is a key issue in all fields of modern science and technology covering microelectronics, photonics, catalysis, biochemical sensors, and so forth.[1−7] In addition to the conventional gas phase, electrochemical and electroless wet chemical deposition methods and other techniques utilizing lasers, ion-beams, and X-rays have also been investigated for incorporating metal clusters onto the substrates in the desired chemical and morphological state(s).[8−21] Use of energetic particle beams and X-rays is particularly attractive since lithographic techniques can also be introduced for patterning/direct-writing purposes. The feasibility of patterning using hard X-rays was demonstrated by Ma et al. and a direct-writing process was reported using vacuum ultraviolet (VUV) both generated by synchrotron sources.[22−24]

Reduction of metal ions while recording XPS (X-ray photoelectron spectroscopy) data was reported in the early days of the development of the technique and is considered as a nuisance.[25−27] However, a recent study reports on the utilization of X-rays and electron beams for inducing in situ oligomerization reactions.[28,29] In addition to X-rays, electron, ion, and other energetic particle exposures, which are frequently encountered for cleaning and/or depth profiling, also cause reduction of certain metal ions to their lower oxidation states and/or preferential removal of oxygen.[30−35] The extent of reduction varies drastically from one metal ion to another, and extensive efforts have been devoted to correlate this with certain chemical/physical properties of the metal ions.[23−35] In our earlier work, we had claimed that the extent of X-ray-induced

* Corresponding author. E-mail: suzer@fen.bilkent.edu.tr.

(1) Henglein, A. *J. Phys. Chem*. **1993**, *97*, 5457.
(2) Mulvaney, P.; Giersing, M.; Henglein, A. *J. Phys. Chem*. **1993**, *97*, 7061.
(3) Wang, Y.; Herron, N. *Science* **1996**, *273*, 632.
(4) Nirmal, M.; Dabbousi, B. O.; Bawendi, M. G.; Macklin, J. J.; Trautman, J. K.; Harris, T. D.; Brus, L. E. *Nature* **1996**, *383*, 802.
(5) Valden, M.; Goodman, D. W. *Science* **1998**, *281*, 1647.
(6) El-Sayed, M. A. *Acc. Chem. Res.* **2001**, *34*, 257.
(7) Kamat, P. V. *J. Phys. Chem. B* **2002**, *106*, 7729.
(8) Xu, X.; Goodman, D. W. *Surf. Sci.* **1993**, *282*, 323.
(9) Rainer, D. R.; Goodman, D. W. *J. Mol. Catal. A* **1998**, *131*, 259.
(10) Martin, H.; Carro, P.; Creus, A. H.; Gonzales, S.; Salvarezza, R. C.; Arvia, A. J. *Langmuir* **1997**, *13*, 100.
(11) Magagnin, L.; Maboudian, R.; Carraro, C. *J. Phys. Chem. B* **2002**, *106*, 401.
(12) Cumberland, S. L.; Strouse, G. G. *Langmuir* **2002**, *18*, 269.
(13) Porter, L. A.; Choi, H. C.; Ribbe, A. E.; Buriak, J. M. *Nano Lett.* **2002**, *2*, 1067.
(14) Rossiter, C.; Suni, I. I. *Surf. Sci.* **1999**, *430*, L553.
(15) Mafune, F.; Kohno, J.; Takeda, Y.; Kondow, T. *J. Phys. Chem. B* **2001**, *105*, 9050.
(16) Sugiyama, M.; Inasawa, S.; Koda, S,; Hirose, T.; Yonekawa, T.; Omatsu, T.; Takami, A. *Appl. Phys. Lett*. **2001**, *79*, 1528. Mini, L.; Giaconia, C.; Amone, C. *Appl. Phys. Lett*. **1994**, *64*, 3404.
(17) Nanai, L.; Hevsi, I.; Bunkin, F. V.; Lukyanchuk, B. S.; Brook, M. R.; Shafeev, A.; Jeiski, D. A.; Wu, Z. C.; George, T. F. *Appl. Phys. Lett*. **1989**, *54*, 736.
(18) Henglein, A.; Meisel, D. *Langmuir* **1998**, *14*, 7392.
(19) Muller, F.; Fontaine, P.; Remita, S.; Faure, M. C.; Lacaze, E.; Goldman, M. *Langmuir* **2004**, *20*, 4791.
(20) Rosenberg, R. A.; Ma, Q.; Lai, B.; Mancini, D. C. *J. Vac. Sci. Technol. B* **1998**, *16*, 3535.
(21) Ila, D.; Williams, E. K.; Zimmerman, R. L.; Poker, D. B.; Hensley, D. K. *Nucl. Instr. Methods B* **2000**, *166−167*, 845.
(22) Ma, Q.; Moldovan, N.; Mancini, D. C.; Rosenberg, R. A. *Appl. Phys. Lett*. **2000**, *76*, 2014.
(23) Divan, R.; Mancini, D. C.; Moldovan, N.; Assoufid, L.; Chu, Y. S.; Ma, Q.; Rosenberg, R. A. *IEEE International Semiconductor Conference CAS*, Sinaia, Romania, 2003; IEEE: Piscataway, NJ, 2003; Vol. 1, p 39.
(24) Caruso, T.; Agostino, R. G.; Bongiomo, G.; Barborini, E.; Piseri, P.; Milani, P.; Lenardi, C.; La Rosa, S.; Bertolo, M. *Appl. Phys. Lett*. **2004**, *84*, 3412.
(25) Walbank, B.; Johnson, C. E.; Main, I. G. *J. Electron Spectrosc.* **1974**, *4*, 263.
(26) Copperthwaite, R. G. *Surf. Interface Anal*. **1980**, *2*, 17.
(27) Storp, S. *Spectrochim. Acta B* **1985**, *40*, 745.
(28) Hernandez, J. E.; Ahn, H.; Whitten, J. E. *J. Phys. Chem. B* **2001**, *105*, 8339.
(29) Ahn, H.; Whitten, J. E. *J. Phys. Chem. B* **2002**, *106*, 11404.
(30) Aduru, S.; Contarini, S.; Rabalais, J. W. *J. Phys. Chem*. **1986**, *90*, 1683.
(31) Kelly, R. *Surf. Sci.* **1980**, *100*, 85.
(32) Malherbe, J. B.; Hofmann, S.; Sanz, J. M. *Appl. Surf. Sci*. **1986**, *27*, 355.
(33) Mitchell, D. F.; Sproule, G. I.; Graham, M. J. *Surf. Interface Anal*. **1990**, *15*, 487.
(34) Brown, N. M. D.; Hewitt, J. A.; Meenan, B. J. *Surf. Interface Anal*. **1992**, *18*, 187.
(35) Fernandez, A.; Espinos, J. P.; Leinen, D.; Gonzalez-Elipe, A. R.; Sanz, J. M. *Surf. Interface Anal*. **1994**, *22*, 111.

10.1021/la0478604 CCC: $30.25
Published on Web 12/02/2004

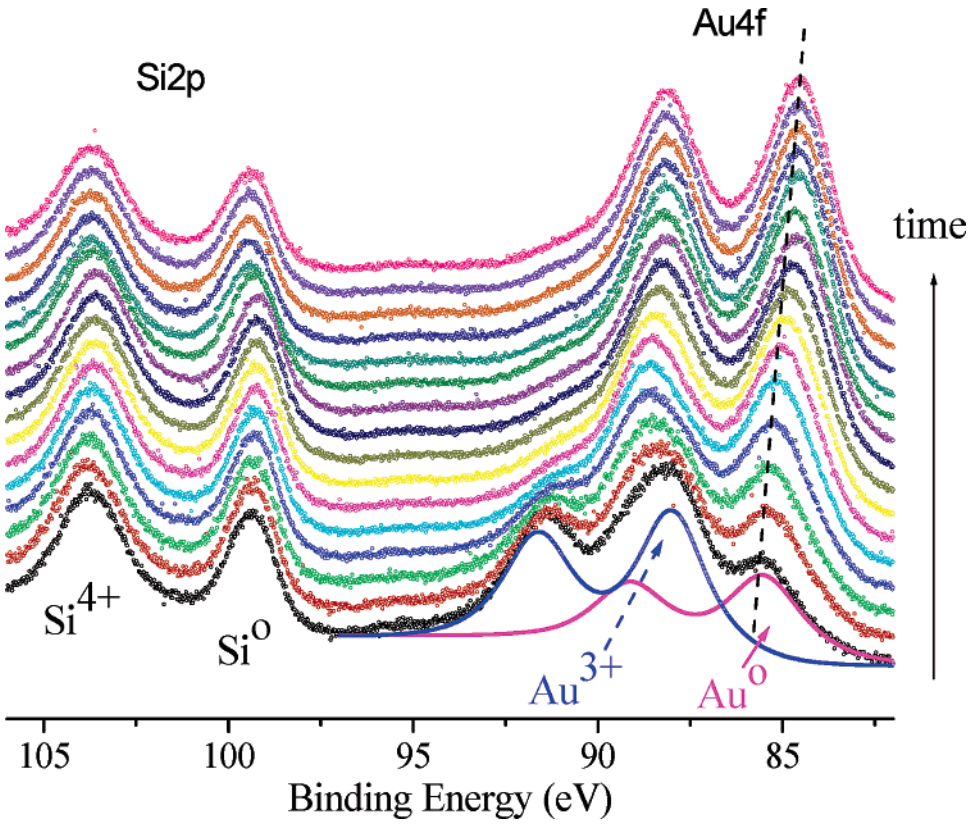

Figure 1. A set of XPS spectra of the $AuCl_4^-/SiO_2$ (4 nm)/Si system recorded as a function of time (ca. 70 h).

reduction could be related to the electrochemical reduction potential of the metal ion.[36,37] Accordingly, gold, having a very high reduction potential of [$\epsilon^0_{red}(Au^{3+}) = 1.5$ V] is one of the most amenable to such changes. Although the process has long been reported, detailed information related to the mechanism such as the nature of the oxidation products and/or the fate of the reduced products (especially whether cluster formation or nucleation also takes place) is not available. From this aspect, XPS is particularly suitable since a significant and measurable chemical shift develops to correlate with the size of gold clusters.[38−42] These are the issues we wish to elaborate in the present contribution. In view of the recent vast interest, the SiO_2/Si substrate and the polymer matrix (poly(methyl methacrylate), PMMA) were chosen to follow the reduction process.[43−47]

Experimental Section

A Si(100) substrate was allowed to stay in concentrated HF solution for 45−60 s to remove native oxide layer and rinsed with deionized water and dried. Clean Si(100) samples were heated in air at 500 °C. The duration of heating was varied from 1 to 4 h to have SiO_2/Si systems with different oxide thicknesses (2−10 nm). After the SiO_2/Si system was prepared, the substrate was dip-coated by a solution containing ~0.03% (w/v) of tetrachloroauric acid and dried in air at room temperature. In the case of the polymer, gold ions were dissolved together with the polymer (PMMA) in acetone and were cast into 10−20 μm films. The thickness of the polymer film was arbitrary but was chosen for clear recording of the IR and/or UV−vis−NIR spectra.

A Kratos ES300 spectrometer with a Mg Kα (not monochromatized) source at 1253.6 eV was used to record the XPS spectra and at the same time to induce the reduction. The reduction process is dose dependent, and normally a higher X-ray dose is preferable for a higher signal-to-noise ratio. However, since one of our objectives was to follow the kinetics of the process a dose as low as possible was needed. As a compromise, a 120 W (15 kV at 8 mA) X-ray dose was used for all the work reported in this contribution. The base pressure was kept below 10^{-8} Torr throughout the measurements. XPS peaks were fitted using the XPSPEAK 4.0 fitting program. Normally the data were recorded at a 90° takeoff angle, but for obtaining depth information lower takeoff angles were also utilized.[48]

In a separate experiment, the polymer films were exposed to 254 nm deep UV radiation using a low-pressure 10 W Hg lamp to induce the reduction within the polymer matrix. The reduction of the ions and subsequent nucleation of the gold particles were followed by a Cary 5E UV−vis−NIR spectrometer.

Results and Discussion

a. Choosing the Reference Point. In all XPS studies, a reference point is required to determine the binding energy changes accurately and the C1s binding energy (at 285.00 eV) of the adventitious carbon is commonly employed. However, to follow the rapid changes in the Au4f level at 84 eV a nearby energy level like Si2p (around 100 eV) is preferable. The use of the Si2p level is itself problematic since it is well-known that the binding energy difference between Si^{4+} and Si^0 increases as the SiO_2

(36) Suzer, S. *Appl. Spectrosc.* **2000**, *54*, 1716.
(37) Suzer, S. *J. Electron Spectrosc.* **2001**, *114−116*, 1151.
(38) Mason, M. G. *Phys. Rev. B* **1983**, *27*, 748.
(39) Zhang, L.; Persand, R.; Madey, T. E. *Phys. Rev. B* **1997**, *56*, 10549.
(40) Luo, K.; Kim, D. Y.; Goodman, D. W. *J. Mol. Catal. A* **2001**, *167*, 191.
(41) Choudhary, T. W.; Goodman, D. W. *Top. Catal.* **2002**, *21*, 25.
(42) Lamber, R.; Wetjen, S.; Schulz-Ekloff, G. *J. Phys. Chem. B* **1995**, *99*, 13834.
(43) Thran, A.; Kiene, M.; Zaporojtchenko, V.; Faupel, F. *Phys. Rev. Lett.* **1999**, *82*, 1903.
(44) Malone, K.; Weaver, S.; Taylor, D.; Cheng, H.; Sarathy, K. P.; Mills, G. *J. Phys. Chem. B* **2002**, *106*, 7422.
(45) Tanaka, H.; Mitsuishi, M.; Miyashita, T. *Langmuir* **2003**, *19*, 3103.
(46) Biswas, A.; Aktas, O. C.; Schurmann, U.; Saeed, U.; Zaporojtchenko, V.; Faupel, F. *Appl. Phys. Lett.* **2004**, *84*, 2655.
(47) Korchev, A. S.; Bozack, M. J.; Slaten, B. L.; Mills, G. *J. Am. Chem. Soc.* **2004**, *126*, 10.
(48) Fulghum, J. E. *Surf. Interface Anal.* **1993**, *20*, 161.

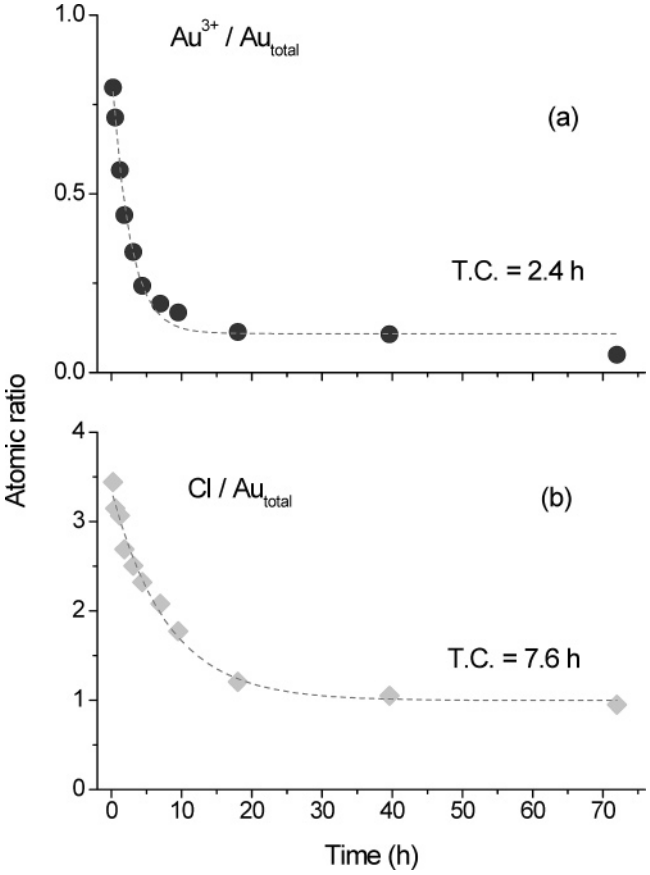

Figure 2. Variation of the atomic ratio of (a) Au^{3+}/Au_{total} and (b) Cl/Au_{total} during the 120 W X-ray exposure. A first-order exponential decay fit to the data gives time constants of 2.7 and 7.6 h for the disappearance of the Au^{3+} and the Cl signals, respectively.

thickness increases. There is a long debate on the factors contributing to these measured binding energy differences such as initial state effects, final state or relaxation effects, charging, and so forth.[49−63] In addition, as we had recently reported, this difference can further be affected by application of a small voltage bias to the sample due to changes in the differential charging between the oxide layer and the Si(m) underneath. We had further reported that the Au4f binding energy shifts are tightly related with the Si2p shifts of the oxide layer rather than the Si(m).[64] In other words, Au4f levels follow faithfully the potential developed on the SiO_2 layer so that the Si2p of the oxide can be taken as the reference.[65]

The other issue is the value of the reference peak (i.e., Si2p of the Si^{4+}). For this purpose, a gold layer is deposited on the SiO_2/Si system using physical vapor deposition with an estimated Au layer ranging from 2 to 10 nm until a uniform gold layer (as judged by scanning electron microscopy (SEM) images) could be grown on the SiO_2/Si system. The extrapolated binding energy difference between Au 4f and Si^{4+} 2p is determined as 19.43 eV. Taking the binding energy of the bulk Au 4f peak as 84.00 eV, we establish the binding energy for the Si^{4+} 2p peak to be 103.43 eV, which will be used as our reference point.

b. X-ray-Induced Reduction of Au^{3+}. As shown in Figure 1, Au^{3+} is reduced to its metallic state during X-ray exposure (ca. 120 W). Increase in the Au^0 peak at the expense of the Au^{3+} peak with time is the fingerprint of the reduction as shown in Figure 2a. The corresponding oxidation process can be followed in the Cl2p region (not shown) which decreases while Au^{3+} is reduced to its metallic state as shown in Figure 2b. It is interesting to note that the intensity of the Cl2p peak decreases but does not diminish completely. Since tetrachloroauric acid is the only source for chloride anions and three chloride anions are oxidized to reduce one gold atom, the intensity of the Cl2p peak should decrease to an intensity ratio of 1 when Au^{3+} reduction is completed. Complete reduction of Au^{3+} to Au occurs after ca. 30 h (at this specific X-ray dose) as the chloride/gold atomic ratio decreases to the expected range (ca. 1). The remaining HCl must somehow be permanently incorporated to the SiO_2 matrix according to the following equation:

$$HAuCl_4(ads) + \text{X-rays} \rightarrow Au(ads) + (3/2)Cl_2(ads) + HCl(ads) \quad (\text{time constant} = 2.4\ \text{h})$$

Hence, within our experimental limits, no other major oxidation products are observed.

Both the variation of the Au^{3+} intensity and the Cl with X-ray exposure exhibit first-order kinetics but with different time constants. Disappearance of gold ions is approximately 3 times faster. This may be surprising since one expects the oxidation and the reduction to proceed simultaneously. However, within our experimental accuracy, we cannot distinguish between the Cl^- and the adsorbed Cl_2 because the binding energy difference between them is too small (<1 eV). Therefore, we interpret this result as the indication that although the oxidation of chloride ions occurs simultaneously with the reduction of gold ions, diffusion of the product, chlorine, out of the substrate into the vacuum takes place with a relatively longer time constant.

$$2Cl^- + \text{X-rays} \rightarrow Cl_2(ads) \quad (\text{time constant} = 2.4\ \text{h})$$

$$Cl_2(ads) \rightarrow Cl_2(g) \quad (\text{time constant} = 7.6\ \text{h})$$

c. Nucleation and Cluster Formation. In addition to the X-ray-induced reduction of Au^{3+}, a shift in the binding energy of Au^0 is also observed as was indicated in Figure 1. The binding energy of gold decreases to that of bulk gold as the particle size of the gold cluster increases and approaches bulk gold.[8,9,38−41] The binding energy difference between Au^0 and Si^{4+} peaks increases from 18.12

(49) Hollinger G.; Jugnet, Y.; Pertosa, P.; Duc, T. M. *Chem. Phys. Lett.* **1975**, *36*, 441.
(50) Grunthaner, F. J.; Grunthaner, P. J.; Vasquez, R. P.; Lewis, B. F.; Maserjian, J.; Madhukar, A. *Phys. Rev. Lett.* **1979**, *43*, 1683.
(51) Grunthaner, F. J.; Grunthaner, P. J.; Vasquez, R. P.; Lewis, B. F.; Maserjian, J.; Madhukar, A. *J. Vac. Sci. Technol.* **1979**, *16*, 1443.
(52) Ishizaka, A.; Iwata, S.; Kamigaki, Y. *Surf. Sci.* **1979**, *84*, 355.
(53) Hollinger, G. *Appl. Surf. Sci.* **1981**, *8*, 318.
(54) Hollinger, G.; Himpsel, F. J. *Appl. Phys. Lett.* **1983**, *44*, 93.
(55) Wagner, C. D.; Joshi, A.; Gulbrandsen, L.; Deal, B. E. *J. Vac. Sci. Technol. B* **1984**, *2*, 107.
(56) Finster, J.; Schulze, D.; Bechstedt, F.; Meisel, A. *Surf. Sci.* **1985**, *152/153*, 1063.
(57) Iqbal, A.; Bates, C. W., Jr.; Allen, J. W. *Appl. Phys. Lett.* **1985**, *47*, 93.
(58) Iwata, S.; Ishizaka, A. *J. Appl. Phys.* **1996**, *79*, 6653.
(59) Zhang, K. Z.; Greeley, J. N.; Banaszak Holl, M. M.; McFeely, F. R. *J. Appl. Phys.* **1997**, *82*, 2298.
(60) Zhang, K. Z.; Banaszak Holl, M. M.; McFeely, F. R. *J. Phys. Chem. B* **1998**, *102*, 3930.
(61) Kobayashi, H.; Kubota, T.; Kawa, H.; Nakato, Y.; Nishiyama, N. *Appl. Phys. Lett.* **1998**, *73*, 933.
(62) Browning, R.; Sobolewski, M. A.; Helms, C. R. *Phys. Rev. B* **1988**, *38*, 13407.
(63) Pasquarello, A.; Hybertson, M. S.; Car, R. *Phys. Rev. B* **1996**, *53*, 10942.
(64) Ulgut, B.; Suzer, S. *J. Phys. Chem. B* **2003**, *107*, 2939.
(65) Karadas, F.; Ertas, G.; Suzer, S. *J. Phys. Chem. B* **2004**, *108*, 1515.

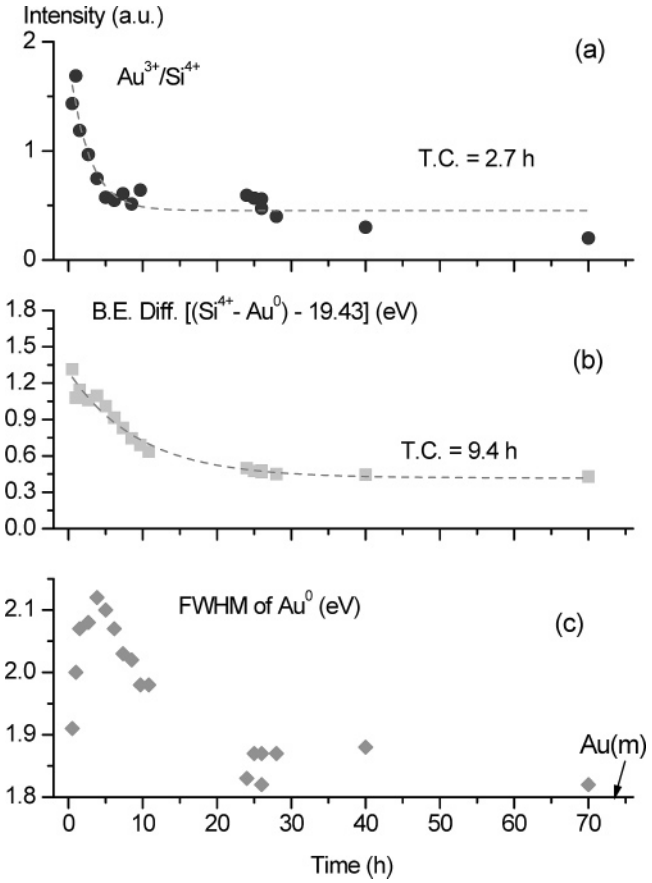

Figure 3. Variation (a) of the intensity of Au^{3+}/Si^{4+} (a first-order exponential decay fit to the data gives a time constant of 2.7 h), (b) in the measured binding energy difference between the Si2p of the oxide (Si^{4+}) and the Au4f of the Au^0 peaks minus the 19.43 eV which corresponds to the difference between the bulk silicon oxide and bulk gold (a first-order exponential decay fit to the data gives a time constant of 9.4 h), and (c) of the fwhm of the Au4f peak corresponding to Au^0.

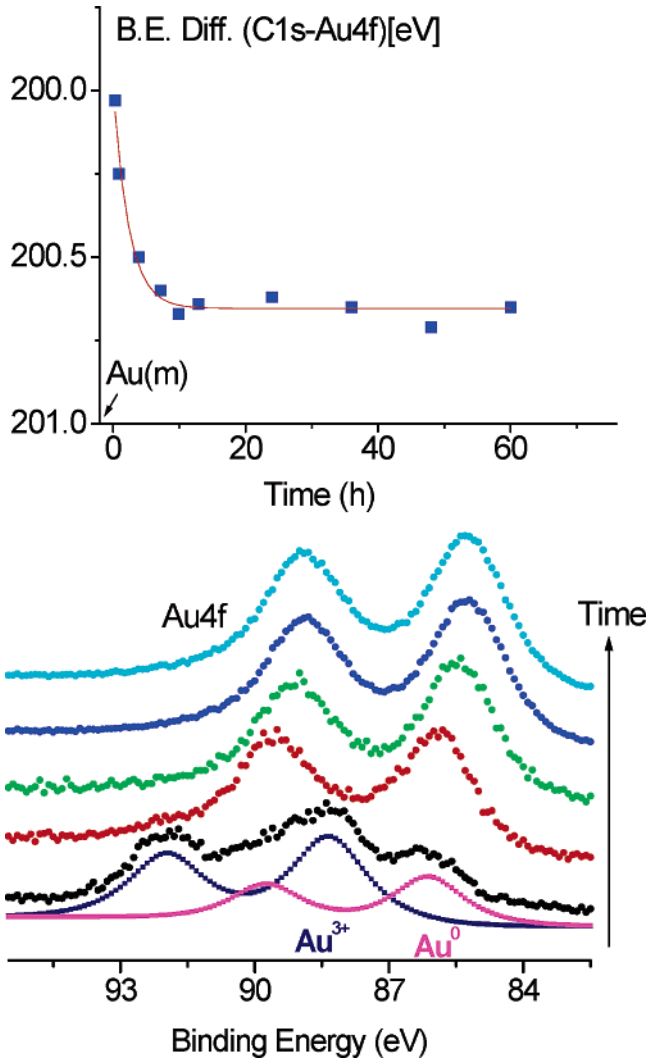

Figure 4. XPS spectra of the $AuCl_4^-$ (PMMA) system recorded as a function of time (ca. 60 h). The variation in the measured binding energy difference between the C1s and the Cl2p peaks is also given as an inset.

to 18.91 eV; hence the binding energy (BE) of gold decreases about 0.8 eV, indicating possibly a nucleation and growth process. When the Si^{4+}2p peak (103.43 eV) is taken as the reference, the BE of Au^0 is calculated as going from 85.31 to 84.52 eV. Goodman et al.[40] reported a similar study where the binding energy of gold, with different gold coverages, was measured. Although Au^0 particles were prepared by the physical vapor deposition method in their study, our gold clusters produced by X-rays gave similar results. In their report, the binding energy of gold cluster changes about 1.8 eV as the gold coverage increases from 0.1 to 25 monolayer (ML). Using the plot depicted by Goodman et al., the average coverage of gold particles obtained from X-ray-induced reduction increases from ~0.1 to ~4 ML in our study. The initial XPS spectrum ($t = 0$) of the gold particles cannot be obtained since X-rays needed to excite photoelectrons also do the reduction. For this reason, the first X-ray photoelectron spectrum where the binding energy of Au^0 is measured as 85.31 eV was obtained after approximately 20 min of X-ray exposure. This is why Goodman et al.[40] measured a binding energy of 85.80 eV for their very small gold nanoparticles that is greater than our initial binding energy of gold particles (85.31 eV) grown by X-ray-induced reduction. This could have been avoided by having rapid scans with sacrifice in the signal-to-noise ratio. As a matter of fact, an initial binding energy of 85.65 eV was obtained after 6 min of X-ray exposure from another sample whose spectrum was obtained with a rapid scan but with poorer signal-to-noise ratio, and hence poorer reliability. In all of our measurements, it is observed that the binding energy of gold particles created by X-rays could not reach the value of the bulk gold (84.00 eV).

In Figure 3, we display the variations in (a) the intensity ratio of Au^{3+}/Si^{4+}, (b) the binding energy difference between the Si^{4+} and Au^0 less 19.43 eV which corresponds to the difference of the bulk gold metal, and (c) the full width at half-maximum (fwhm) of the Au^0 peak, as a function of the X-ray exposure measured all in one experiment. Disappearance of gold ions is similar to the one depicted in Figure 2a with a slightly different time constant. This is not unexpected since it is a different experiment with a different gold ion concentration and so forth. The binding energy difference which we now relate to the growth of the gold nanoparticles also displays a first-order kinetics as shown in Figure 3b with a slower time constant of 9.4 h, indicating again that the kinetics of the nucleation is slower than that of the reduction. It is interesting to note that almost the same factor of difference (3) is measured between the rates of reduction and disappearance of the oxidation product (chlorine gas) and that of the gold nanoparticle growth, pointing out that both of the latter two processes are diffusion controlled.[10]

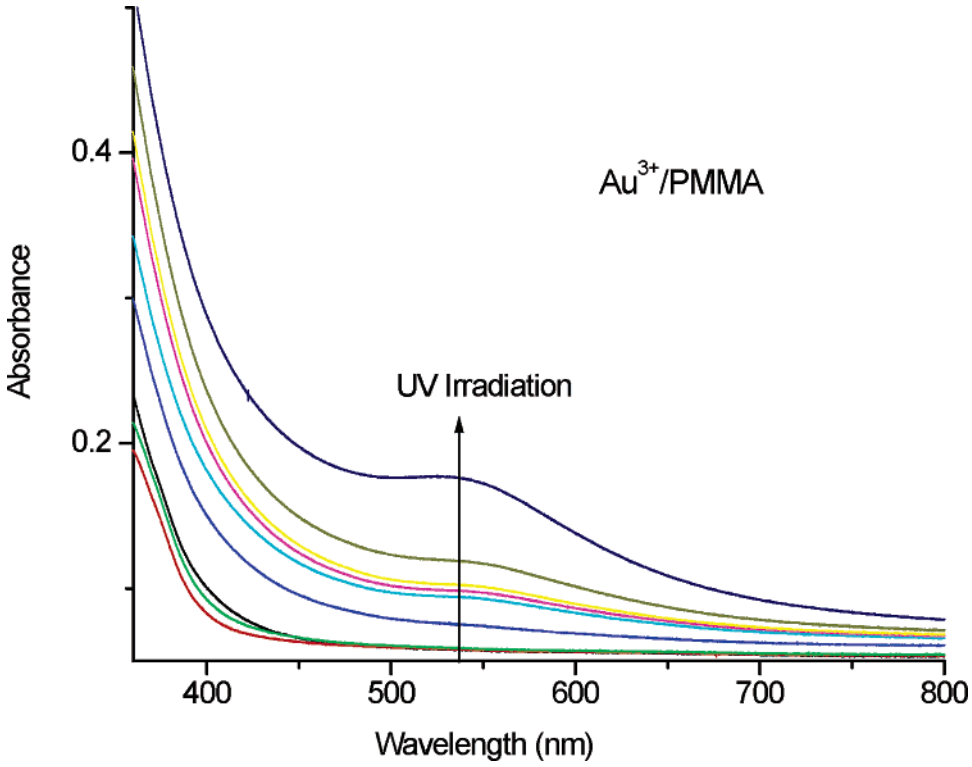

Figure 5. A set of UV−vis−NIR absorption spectra of a 20 μm film of PMMA containing gold salt exposed to deep nm UV radiation.

The fwhm of the gold nanoclusters can also be used to extract some information as shown in Figure 3c. Accordingly, as the reduction and nucleation take place the fwhm initially grows, passes through a maximum, and declines to the value of the bulk gold (1.8 eV) with more or less the same time constant as the growth process. Initially gold atoms are isolated, and as they start to grow randomly into clusters their heterogeneity increases (as displayed by increased width) to a point, after which the particles mature and approach the bulk behavior.

d. Reduction in Polymer Matrix. To test the generality of the process, we have also investigated the reduction of gold in a polymer (PMMA) matrix. PMMA was chosen for its widespread use in microelectronic fabrication. Figure 4 depicts the Au4f region of the film recorded consecutively. Since gold ions are distributed throughout the entire polymer matrix, the signal-to-noise ratio is poorer. The results, however, are the same as on the SiO_2/Si substrate that X-ray-induced reduction and subsequent nucleation take place also in the polymer matrix. This time the binding energy difference between the Au4f and C1s was monitored as also shown in Figure 4. Again, the difference is 0.3 eV short of the bulk value of the gold metal, supporting the finding that nanoclusters of gold are also formed within the polymer matrix. The 0.3 eV difference is smaller than the 0.5 eV we measured for the gold clusters on the oxide matrix. However, considering the fact that the accuracy of measuring the binding energy difference in the polymer case is less (since we are forced to use the C1s as the reference) we cannot state that they are significantly different. To clarify this point, the process was also followed in air using 254 nm deep UV light for inducing the reduction. Figure 5 depicts the UV−vis−NIR absorption spectra of the films. Here again gold nanocluster formation is evidenced by the increase of absorption around 530 nm, supporting the similarity of the processes on the oxide and in the polymer matrix.[66−69]

Conclusions

The main emphasis of this work was a detailed investigation of the X-ray-induced reduction of gold ions deposited from an aqueous solution onto a silicon oxide substrate or in a polymer matrix in vacuum. The corresponding major oxidation product is determined as chlorine gas, which initially is adsorbed on the surface but eventually diffuses out into the vacuum. Both the reduction of the gold ions and the disappearance of the chlorine follow a first-order kinetics in time, but the former is approximately 3 times faster. The reduction process is also followed by the growth of gold nanoparticles as evidenced by the decrease in the binding energy and the changes in the width of the Au4f peak corresponding to Au^0. Here also the change in the binding energy displays a first-order kinetics again approximately 3 times slower than the reduction process. Hence, both the disappearance of the chlorine and growth of the gold nanoclusters are diffusion controlled. Both on the oxide support and within the polymer matrix, the measured binding energy of the Au^0 particles cannot reach the bulk value, which supports the findings that gold particles prefer to grow three-dimensionally (islandlike model) rather than two-dimensionally.[10] A similar process was also carried out in air by 254 nm deep UV irradiation of a PMMA film containing gold salt, leading also to reduction and nanocluster formation evidenced by UV−vis−NIR absorption spectroscopy.

(66) Alvarez, M. M.; Khoury, J. K.; Schaaff, T. G.; Shafigulin, M. N.; Vezmar, I.; Whetten, R. L. *J. Phys. Chem. B* **1997**, *101*, 3706.
(67) Taleb, A.; Petit, C.; Pileni, M. P. *J. Phys. Chem. B* **1998**, *102*, 2214.
(68) Templeton, A. C.; Pietron, J. J.; Murray, R. W.; Mulvaney, P. *J. Phys. Chem. B* **2000**, *104*, 564.
(69) Shipway, A. N.; Lahav, M.; Gabai, R.; Willner, I. *Langmuir* **2000**, *16*, 8789.

As a final conclusion, we state that both X-rays and UV radiation lead to reduction of gold ions deposited from solutions (as opposed to gas-phase deposition), followed by formation of gold nanoclusters which can easily be used for lithographic and/or patterning/direct-writing purposes with especially strong synchrotron sources.

Acknowledgment. This work was supported by TUBA (Turkish Academy of Sciences) and by TUBITAK (The Scientific and Technical Research Council of Turkey) through Grant No. TBAG-2261.

LA0478604